

Hydrogeologic Assessment of the Battelle West Jefferson Former North Nuclear Site
December 10, 2007

Prepared by M. Kelley¹, CPG, CGWP

Introduction

The former North Nuclear Site (North Site) at Battelle's West Jefferson facility, located in West Jefferson Ohio, has been licensed by the U.S. Nuclear Regulatory Commission (NRC) to store and use regulated quantities of nuclear materials to conduct research on nuclear fuel and reactor processes for the U.S. government and other clients. Separate from its NRC license, Battelle also performed research at the site for the U.S. Department of Energy (DOE). Nuclear-related research operations at the West Jefferson North Site ceased in 1986 and the North Site has since been undergoing surveillance and maintenance and decontamination and decommissioning (D&D). Figure 1 is a site map of North Site prior to D&D activities. Except for a few remaining structures that support current (non-nuclear) activities, the historical site infrastructure that was associated with nuclear activities has been demolished and removed, including soil containing radiological materials released during historical site activities. The goal of the D&D process is to return the site to a condition that is suitable for unrestricted use. Furthermore, current and planned activities at the North Site do not involve nuclear-related activities; therefore, Battelle is seeking to terminate its NRC license.

As part of the D&D program, the U.S. Environmental Protection Agency (U.S. EPA) and the Ohio EPA reviewed historical environmental characterization data and commented on the dose modeling that was performed to demonstrate that residual levels of radiological materials remaining in the subsurface at the site following cleanup operations is consistent with an unrestricted future land use objective. Specifically, the Ohio EPA suggested that the dose modeling, which evaluated risk from exposure to groundwater in the lower part of the glacial overburden (i.e., in the "805"² layer) was too limited and should be expanded to evaluate potential risks associated with shallower groundwater at the site, namely in the "855" and "885" layers which occur in the middle and upper part of the glacial overburden, respectively. These upper zones were not evaluated in the original dose modeling because it was believed that they were not laterally extensive or hydraulically capable of providing sufficient yield to support an on-site or off-site groundwater exposure scenario (e.g., drinking water well, irrigation well).

Battelle's Environmental Safety and Health (ESH) department is responsible for supporting the Nuclear Regulatory Commission (NRC) in the D&D and license termination process. In response to Ohio EPA's comments on the dose modeling, ESH requested an independent review of the geology of the North Site to determine if there is evidence of shallow water-bearing zones that could support a drinking water receptor. This memorandum summarizes the results of the assessment.

¹ Battelle, 505 King Ave., Columbus, OH. 43201 kelleym@battelle.org

² Terminology: 805, 855, and 885 'layers' refers to the approximate elevation (ft, above mean sea level) where sand was encountered during historical soil borings at the site. The term "layer" is used for convenience but does not necessarily imply a single laterally extensive zone.

Objectives

The primary objective of this assessment was to evaluate geologic data from the site to determine if sediments are present that could support a water-bearing zone and/or that could transport groundwater off site; and if such deposits are present, to map their distribution and lateral continuity. Previously, the geology of the site has been conceptualized to include three sand zones within a thick deposit of glacial overburden that is comprised mostly of clay overlying limestone bedrock (Figure 2). The three sand layers have been referred to as the 885, 855, and 805 layers based on their approximate elevation. A key question in this study was whether sand is present at these elevations in laterally continuous zones or if it occurs in isolated disconnected lenses. The Ohio EPA has suggested that the 855 zone especially may be laterally continuous beneath the site and possibly extend off-site.

Methods

To evaluate the distribution and continuity of potentially transmissive deposits at the site, soil boring data from historical investigations were compiled and used to map the three dimensional distribution of sand at the site (any deposits that contained gravel were combined with the sand). Sources of soil boring data include Battelle (1990a and 1990b), Bowser Morner (2006), DLZ (2002a, 2002b, and 2003), and Miller et al. (1997). The 3D mapping was performed using a geospatial modeling program – EarthVision® version 7.5 (www.dgi.com) – which employs contouring algorithms that were used predict the shape of the sand bodies in three-dimensional space. Use of a computer program for this purpose was preferred over manual interpretation to allow for a more rigorous and consistent interpretation. Even with a computer program, however, uncertainty exists in the data interpretation. Therefore, two interpretations of the sand distribution were produced. The first interpretation is considered the most realistic; whereas, the second interpretation favors the likelihood that sand bodies are connected.

Results

Sand Distribution

Figures 3a and 3b are 2D site maps showing the modeled lateral distribution of sand beneath the site, as predicted using Earth Vision® and contouring options 1 and 2, respectively. Both interpretations indicate that sand is present in the center of the site and along the eastern boundary of the site in the vicinity of the former filter beds adjacent to Darby Creek. Note that in Figure 3a, these two sand areas are separated by a discontinuity; whereas, in Figure 3b, these two sands are connected.

Figures 4a and 4b show the modeled lateral distribution of sand in the shallow glacial overburden, above an elevation of 865 ft amsl (land surface near the center of the site is approximately 910 ft amsl). It is apparent that there is very little sand in this interval; and, the sand that is present occurs in isolated lenses according to both contouring interpretations. These data suggest that the uppermost ~45 ft of glacial overburden is dominated by non-sand deposits (i.e., clay, silt) and that a continuous sand layer (i.e., 885) is not present in this interval.

Figures 5a and 5b show the modeled lateral distribution of sand in the middle portion of the glacial overburden, between an elevation of 830 ft amsl and 865 ft amsl (approximate depths of 45 to 80 ft below ground surface (bgs)). Sand is abundant in this middle interval, and the strong similarity of these figures to Figures 3a and 3b indicate that the majority of sand in the glacial overburden occurs in this interval. The two contouring interpretations provide similar results except that the second contouring interpretation suggests that sand is slightly more extensive beneath the site (for example, note that sands in the middle and eastern part of the site “connect” in Figure 5b).

Figures 6a and 6b show the modeled lateral distribution of sand in the lower glacial overburden, below an elevation of 830 ft amsl (below a depth of approximately 80 ft bgs). This zone is bounded on the bottom by limestone bedrock. Sand is relatively scarce in this interval occurring in isolated lenses according to both contouring interpretations. These data suggest that the lower glacial overburden is dominated by non-sand materials and that a laterally continuous sand layer (i.e., 805 layer) isn't present in this interval.

Figures 7a and 7b are 3D illustrations of the sand deposits beneath the site, created using Earth Vision[®] and contouring interpretations 1 and 2, respectively. Note the isolated lenses of sand in the upper and lower portions of the section in contrast to the more extensive sand in the middle section. The limestone surface is shown beneath the glacial overburden as defined by soil borings at the site.

Figure 8 is a 2D cross section view through the site, along line A-A' (see Figure 1 for location of A-A'). This figure illustrates the depths where sand was detected in all of the soil borings (note: all soil borings at the site have been projected onto this cross section; a few are labeled for reference). The cluster of borings along the eastern edge of the cross section are mostly CPT (Cone penetrometer technology) points from Miller et al. (1997). For reference, three horizontal lines have been drawn through the cross section at elevations of 885, 855, and 805 ft amsl. Sand is represented by orange/red color. From this, it is again apparent that the majority of sand occurs in the middle portion of the glacial overburden. It is also apparent that fewer borings penetrated the lower glacial overburden; therefore, there is a potential for underestimating the amount of sand in this interval. In contrast, the greatest number of soil borings penetrated the shallow glacial overburden; therefore, there is less uncertainty associated with this interval.

Figures 9a and 9b are cross sections along line B-B' (see Figure 1), showing contour interpretations 1 and 2, respectively of the sand distribution along this line. This section crosses the site in the same location as Ohio EPA's cross section NW-SE (see facsimile sent to Battelle September 26, 2007). Both contour interpretations (Figures 9a and 9b) suggest that sand is not laterally continuous beneath the site at this location. Note that Ohio EPA's interpretation suggests that sand in the middle portion of the section is laterally continuous across the site at this location.

Figures 10a and 10b show the modeled sand distribution in 2D cross-section view along transect C-C' (Figure 1). This section crosses the site further south than B-B' and in the same location as Ohio EPA's cross section W-S (see facsimile sent to Battelle September 26, 2007). More sand is

present in this portion of the site, in particular in the middle part of the glacial overburden. Contouring interpretation 2 suggests that the sand may be laterally continuous nearly to Darby Creek (note: a transect just north of this location would show sand extending all the way to Darby Creek; however, this transect falls slightly outside the area with data coverage as it approaches Darby Creek).

Hydraulic Conductivity Data

Hydraulic conductivity data obtained in several historical site investigations were compiled and are summarized on Table 1. Sources of information for the hydraulic conductivity data include Battelle (1990a and 199b) [for wells installed in 1989/1990], DLZ (2002a, 2002b, and 2003) [for wells installed in 2002/2003], and Bowser Morner (2006) [for wells installed in 2006]. All hydraulic conductivity data were obtained by conducting slug tests on individual monitoring wells; no pumping tests were performed. Duplicate tests were performed on many wells. In the references cited above, hydraulic conductivity values were derived for each well by interpreting slug test data using standard methods including Hvorslev, Bouwer and Rice, and Cooper et al. The derived hydraulic conductivity values represent the hydraulic conductivity of the sediments adjacent to the screened interval of the well. On Table 1 below, the hydraulic conductivity results have been sorted into three categories labeled 885, 855, and 805, based on the elevation of the well's screened interval.

Statistical analyses of the data show that the data are lognormally distributed; therefore, the geometric mean provides a better representation of the central tendency value than the arithmetic mean. The middle portion of the glacial overburden (i.e., 855 layer) has the highest overall geometric mean hydraulic conductivity (1.68E-04/1.93E-04 cm/sec), which is slightly greater than the geometric mean of the lower glacial overburden (i.e., 805 layer) (9.25E-04/8.84E-04 cm/sec) and the upper glacial overburden (i.e., 885 layer) (4.71E-05/5.92E-05 cm/sec). These data are shown graphically in Figure 11. It is important to realize that the hydraulic conductivity values presented here are biased toward the coarser-grained deposits (i.e., sand and gravel) because the hydraulic conductivity data were derived from monitoring wells which were designed to be completed in these types of deposits rather than finer-grained, less permeable materials.

Table 1. Summary of Hydraulic Conductivity Data

Layer	Data	N	Mean	St. Dev.	Median	Minimum	Maximum	Geometric Mean
			cm/sec	cm/sec	cm/sec	cm/sec	cm/sec	cm/sec
all layers	all	72	2.51E-03	1.36E-02	1.30E-04	4.20E-09	1.13E-01	9.09E-05
	averaged	42	3.80E-03	1.77E-02	1.11E-04	1.42E-07	1.13E-01	1.01E-04
885	all	24	1.69E-03	4.97E-03	1.65E-04	4.20E-09	2.40E-02	4.71E-05
	averaged	15	2.16E-03	6.18E-03	9.50E-05	1.42E-07	2.40E-02	5.92E-05
855	all	25	5.49E-03	2.26E-02	1.36E-04	4.14E-06	1.13E-01	1.68E-04
	averaged	15	8.39E-03	2.91E-02	1.28E-04	4.87E-06	1.13E-01	1.93E-04
805	all	23	1.26E-04	8.40E-05	1.28E-04	8.80E-06	2.81E-04	9.25E-05
	averaged	12	1.22E-04	1.22E-04	1.12E-04	1.21E-05	2.74E-04	8.84E-05

Note: "Averaged" indicates that duplicate test results for an individual well were averaged before calculating summary statistics

Groundwater Flow Direction

Groundwater level measurements were collected in October 2007 to map the direction of groundwater movement at the site. Figure 1 shows a water-table contour map for wells in the uppermost glacial overburden, with arrows indicating general direction of groundwater movement (i.e., only data from wells screened in the upper [approximately 15 ft] of glacial overburden were used to construct this map). As shown, groundwater in the shallow glacial overburden has a potential to flow laterally toward the lake following land surface topography. Figure 12 is a 2D cross section view along transect A-A' that shows the general pattern of vertical groundwater flow. There is a clear downward hydraulic gradient from the water-table surface to the middle portion of the glacial overburden. At this depth, there is a greater potential for groundwater to move laterally than vertically. The direction of groundwater flow is to the east toward Darby Creek. Near Darby Creek, there is an upward hydraulic gradient, indicating that groundwater probably discharges to the creek rather than flowing beneath/past the creek (this conclusion is not definitive as water-level data from the opposite side of the creek would be needed to confirm). Based on these data, groundwater that infiltrates through the upper glacial overburden probably flows laterally primarily through the middle and lower portion of the glacial overburden toward and eventually into Darby Creek. A flow budget has not been developed to quantify the amount of infiltration that penetrates the upper glacial overburden and reaches the middle/lower glacial overburden.

Summary and Conclusions

At the West Jefferson North Site, section of glacial overburden approximately 100 feet thick overlies limestone bedrock. The glacial overburden contains a mix of deposits ranging from low-permeability clay to sand and gravel. Groundwater occurs at a relatively shallow depth (a few to several feet below ground surface), indicating that nearly the entire section is saturated. The three-dimensional distribution of the coarse-grained deposits (i.e., sand and gravel) within the glacial overburden were mapped using historical soil boring data and a geospatial computer modeling program. The results show that sand is sparse in the upper and lower glacial overburden but common in the middle section. Further, the sand in the middle section appears to be laterally continuous, extending from beneath the area that was formerly occupied by buildings to Darby Creek, thus providing a potential conduit for groundwater to flow from beneath the site to the creek. The amount of groundwater that infiltrates through the upper glacial overburden and reaches the middle/lower glacial overburden where it can move laterally has not been quantified.

References

- Battelle, 2006. West Jefferson North Facility: Monitoring Well Cluster Location Plan. A Limited Field Investigation to Address Current Uncertainties in the Flow System and Water Quality. Battelle Internally Sponsored Study. August 3.
- Battelle, 1990a. Site Characterization West Jefferson North Site Groundwater Monitoring Well Hydraulic Conductivity Testing and Analysis (January 31, 1990)
- Battelle, 1990b. Geology and Hydrogeology of West Jefferson North Site (September 14, 1990)
- Bowser Morner, 2006. Groundwater Monitoring Well Installations at the Battelle West Jefferson North Site West Jefferson, Ohio (October 30, 2006)
- DLZ, 2003a. Data Report Spring 2003 - Well Installation and Geotechnical Testing West Jefferson North Site (September 5, 2003).
- DLZ, 2003b. Data Report Fall 2002 - Well Installation and Geotechnical Testing West Jefferson North Site (March 17, 2003)
- DLZ, 2002. Well Installation and Geotechnical Testing West Jefferson North Site (September 24, 2002)
- Miller, S.F., M.D. Thompson, M.A. Glennon, B.E. Davies, M.A. Benson, C.A. Padar, L.D. McGinnis, and J. Paulson, 1997. Assessing Environmental Risk of the Retired Filter Bed Area, Battelle West Jefferson. Contribution of Center for Environmental Restoration Systems, Energy Systems Division, Argonne National Laboratory. Sponsored by United States Department of Energy, Columbus Environmental Management Project and Chicago Operations Office (April, 1997).

List of Figures

- Fig 1. Site Map Showing Wells, Hydrogeologic Cross Sections, and Water Table Map of Shallow Groundwater Based on Water Levels Measured October 2007
- Fig 2. Site Geology – Idealized
- Fig 3a. Modeled Distribution of Sand/Gravel in Glacial Overburden Based on Boring Log Data – Contouring Option 1
- Fig 3b. Modeled Distribution of Sand/Gravel in Glacial Overburden Based on Boring Log Data – Contouring Option 2
- Fig 4a. Modeled Distribution of Sand/Gravel in Glacial Overburden Above 865-ft, amsl Based on Boring Log Data – Contouring Option 1
- Fig 4b. Modeled Distribution of Sand/Gravel in Glacial Overburden Above 865-ft, amsl Based on Boring Log Data – Contouring Option 2
- Fig 5a. Modeled Distribution of Sand/Gravel in Glacial Overburden Between 830 and 865-ft, amsl Based on Boring Log Data – Contouring Option 1
- Fig 5b. Modeled Distribution of Sand/Gravel in Glacial Overburden Between 830 and 865-ft, amsl Based on Boring Log Data – Contouring Option 2
- Fig 6a. Modeled Distribution of Sand/Gravel in Glacial Overburden Below 830 ft, amsl Based on Boring Log Data – Contouring Option 1
- Fig 6b. Modeled Distribution of Sand/Gravel in Glacial Overburden Below 830 ft, amsl Based on Boring Log Data – Contouring Option 2
- Fig 7a. 3D Perspective of Modeled Sand/Gravel Distribution in Glacial Overburden – Contouring Option 1
- Fig 7b. 3D Perspective of Modeled Sand/Gravel Distribution in Glacial Overburden – Contouring Option 2
- Fig 8. Composite Cross Section Through Site Showing Sand/Gravel Detected in Boring Logs (All Soil Borings Shown)
- Fig 9a. Cross Section B-B' Showing Modeled Distribution of Sand/Gravel – Contouring Option 1 (Note: this Section Crosses the Site in the Same Location As OEPA Cross Section NW-SE)
- Fig 9b. Cross Section B-B' Showing Modeled Distribution of Sand/Gravel – Contouring Option 2 (Note: this Section Crosses the Site in the Same Location As OEPA Cross Section NW-SE)
- Fig 10a. Cross Section C-C' Showing Modeled Distribution of Sand/Gravel – Contouring Option 1 (Note: this Section Crosses the Site in the Same Location As OEPA Cross Section W-E)

Fig 10b. Cross Section C-C' Showing Modeled Distribution of Sand/Gravel – Contouring Option 2 (Note: this Section Crosses the Site in the Same Location As OEPA Cross Section W-E)

Fig 11. Probability Distribution Plots of Hydraulic Conductivity Data

Fig 12. Cross Section Through Site Showing Direction of Groundwater Movement (Based on Water Level Measurements Collected October, 2007)

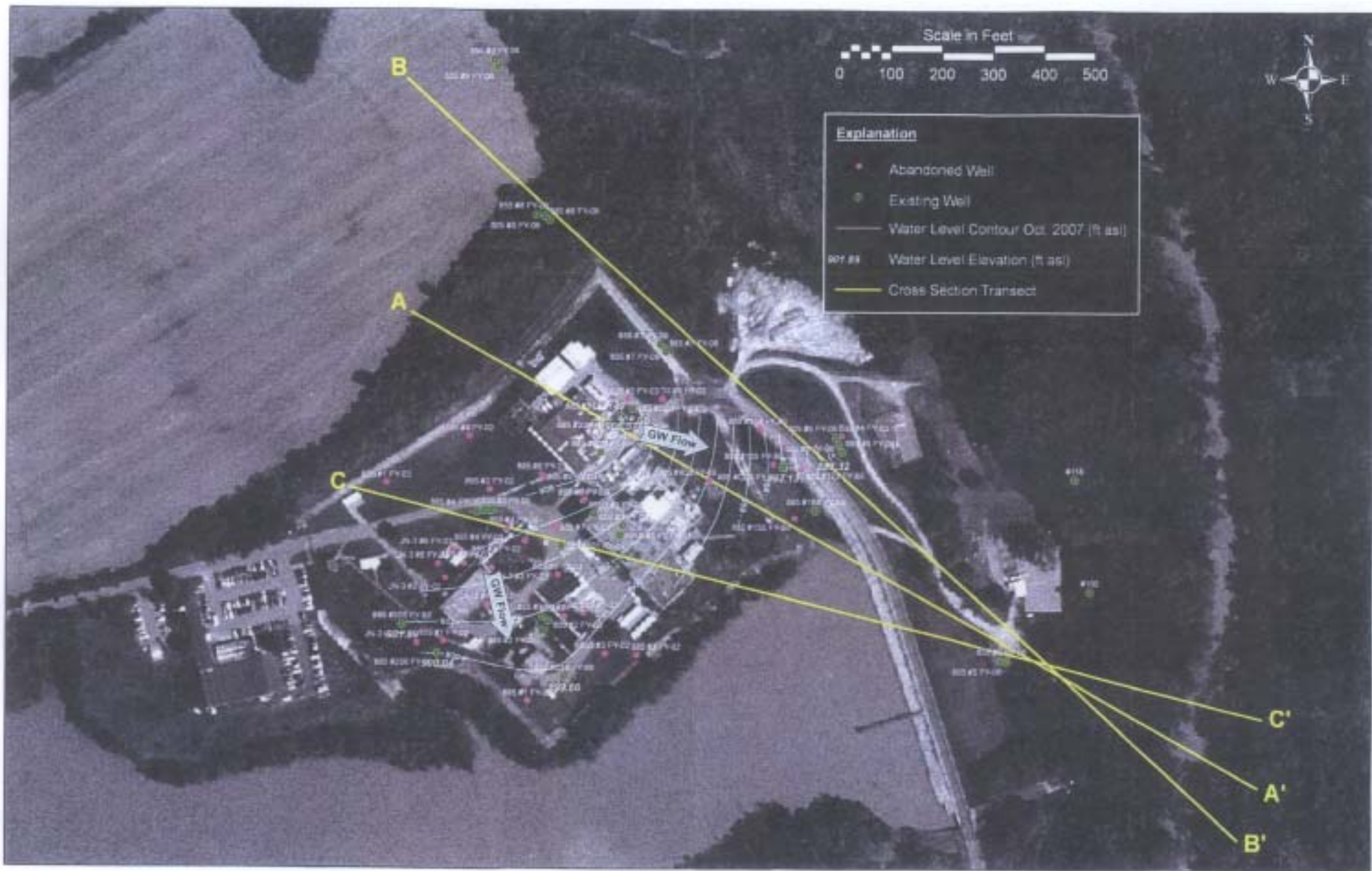
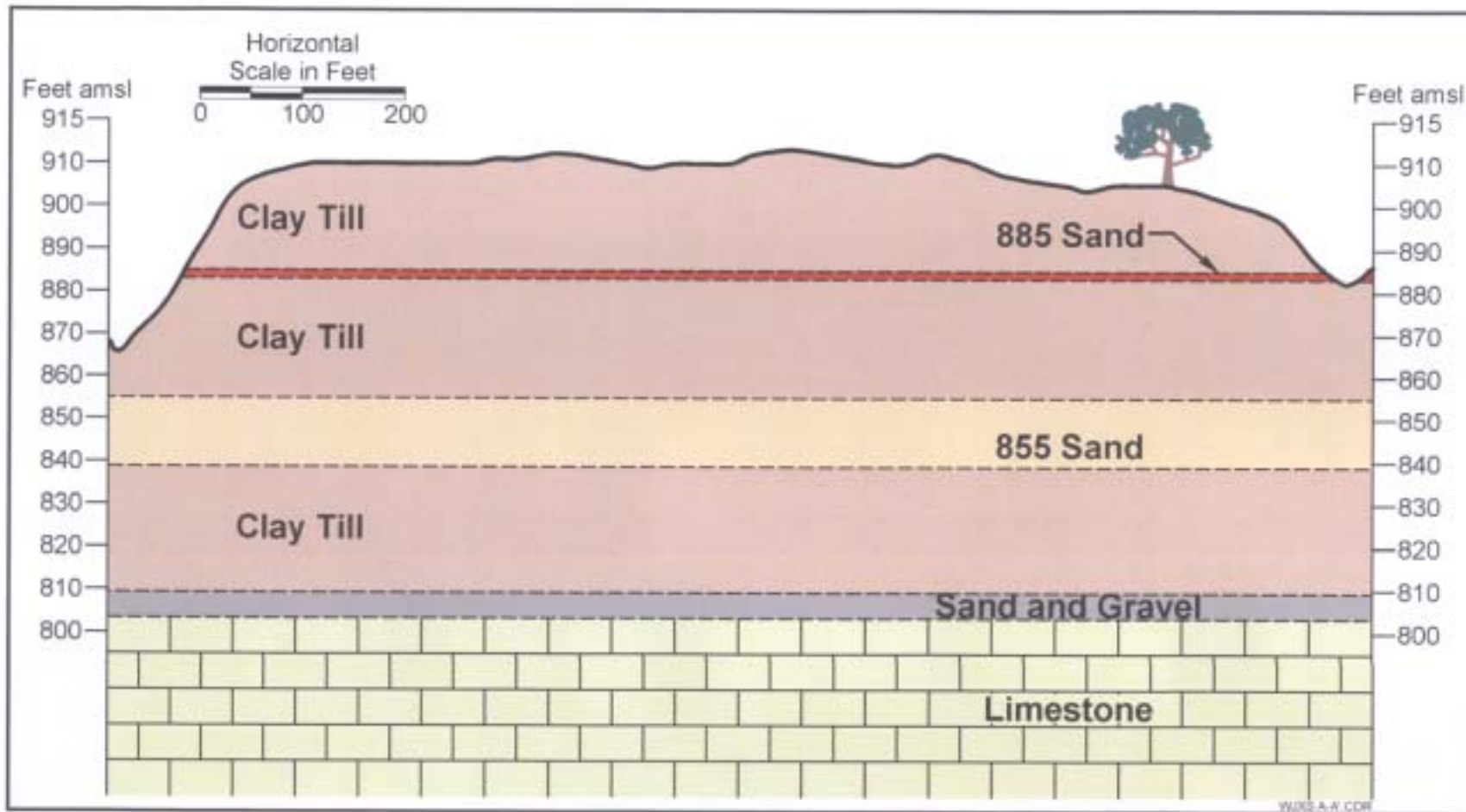


Fig 1. Site Map Showing Wells, Hydrogeologic Cross Sections, and Water Table Map of Shallow Groundwater Based on Water Levels Measured October 2007



Source: Battelle (2006)

Fig 2. Site Geology - Idealized

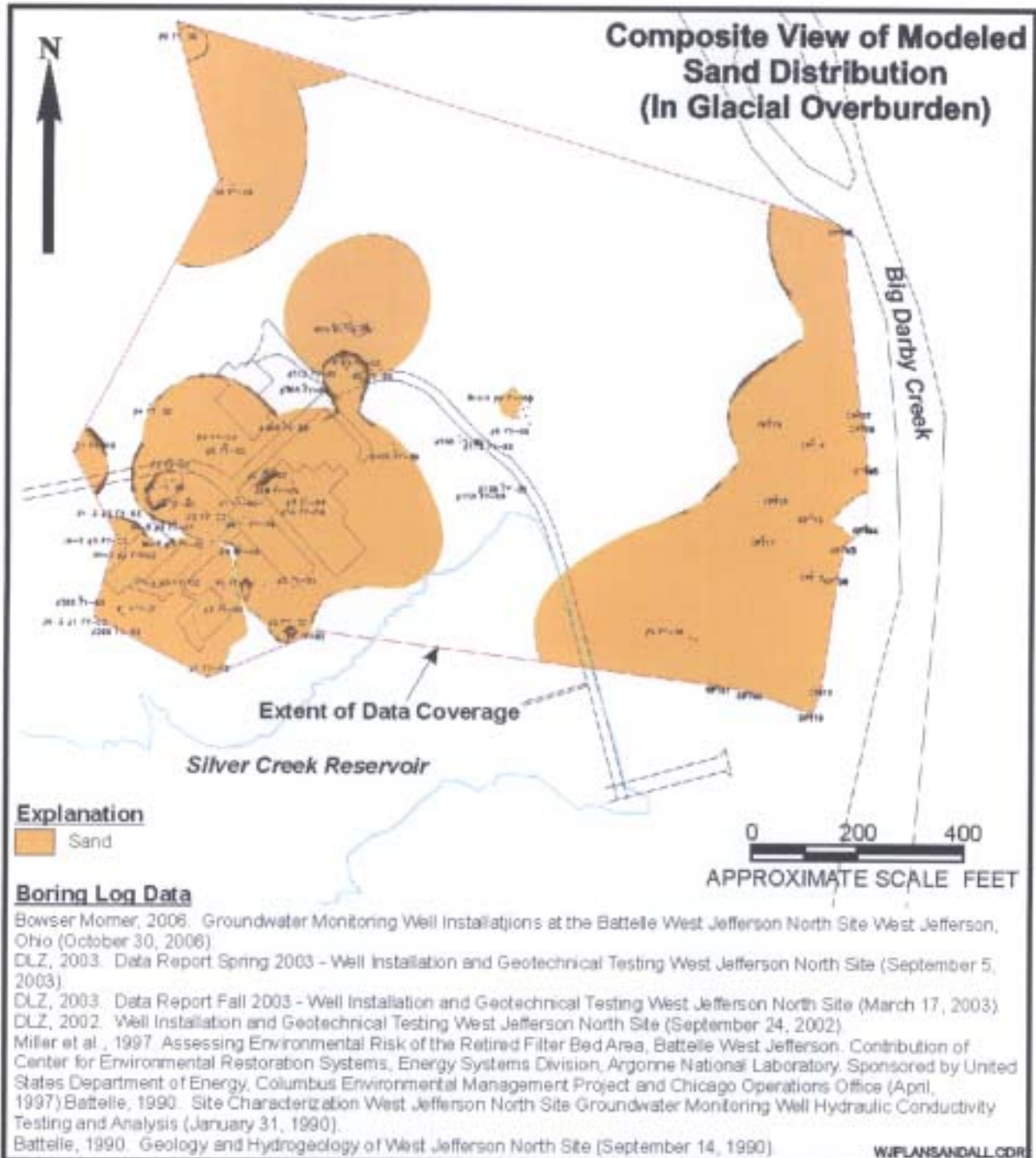


Fig 3a. Modeled Distribution of Sand/Gravel in Glacial Overburden Based on Boring Log Data – Contouring Option 1

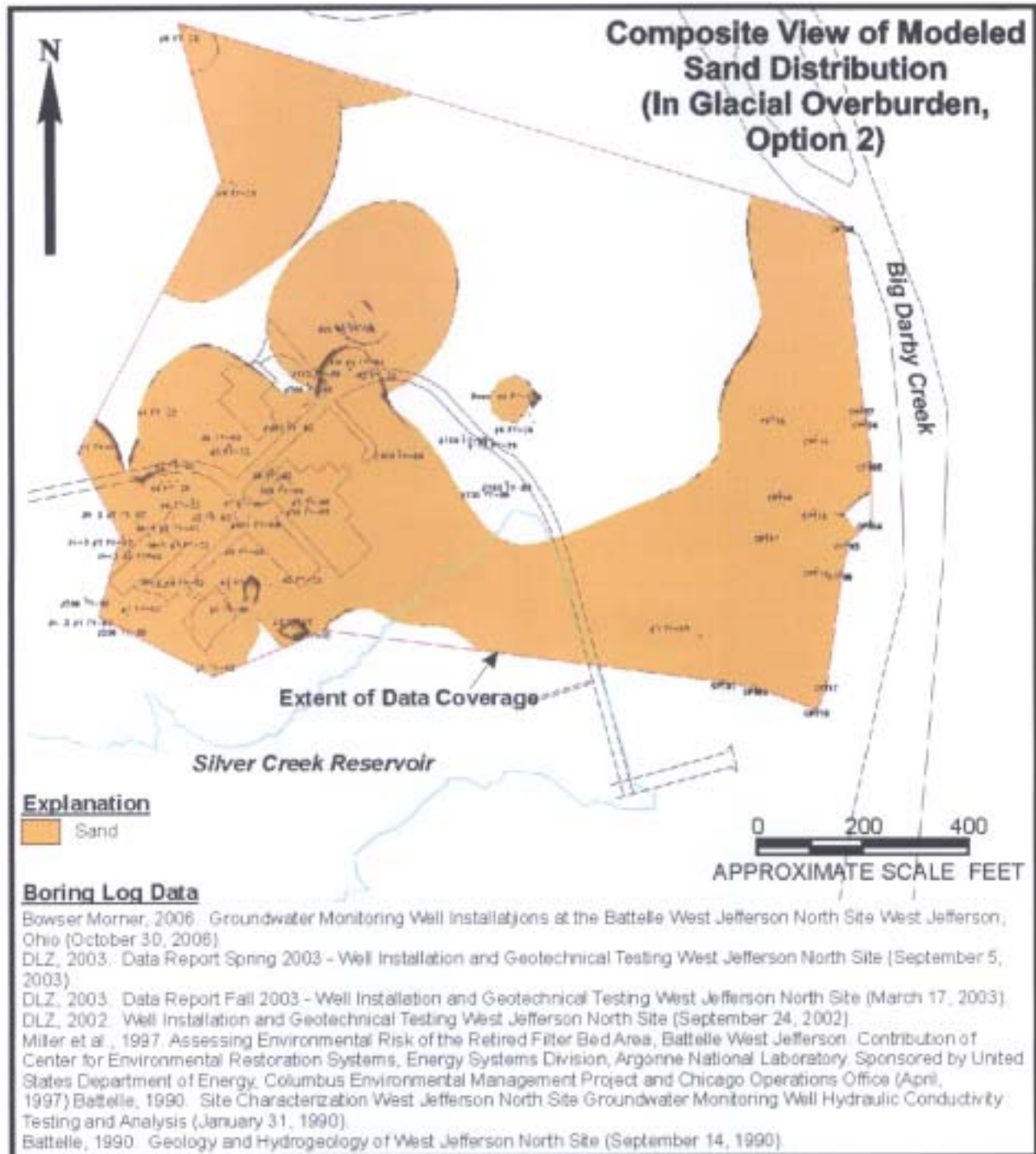


Fig 3b. Modeled Distribution of Sand/Gravel in Glacial Overburden Based on Boring Log Data – Contouring Option 2

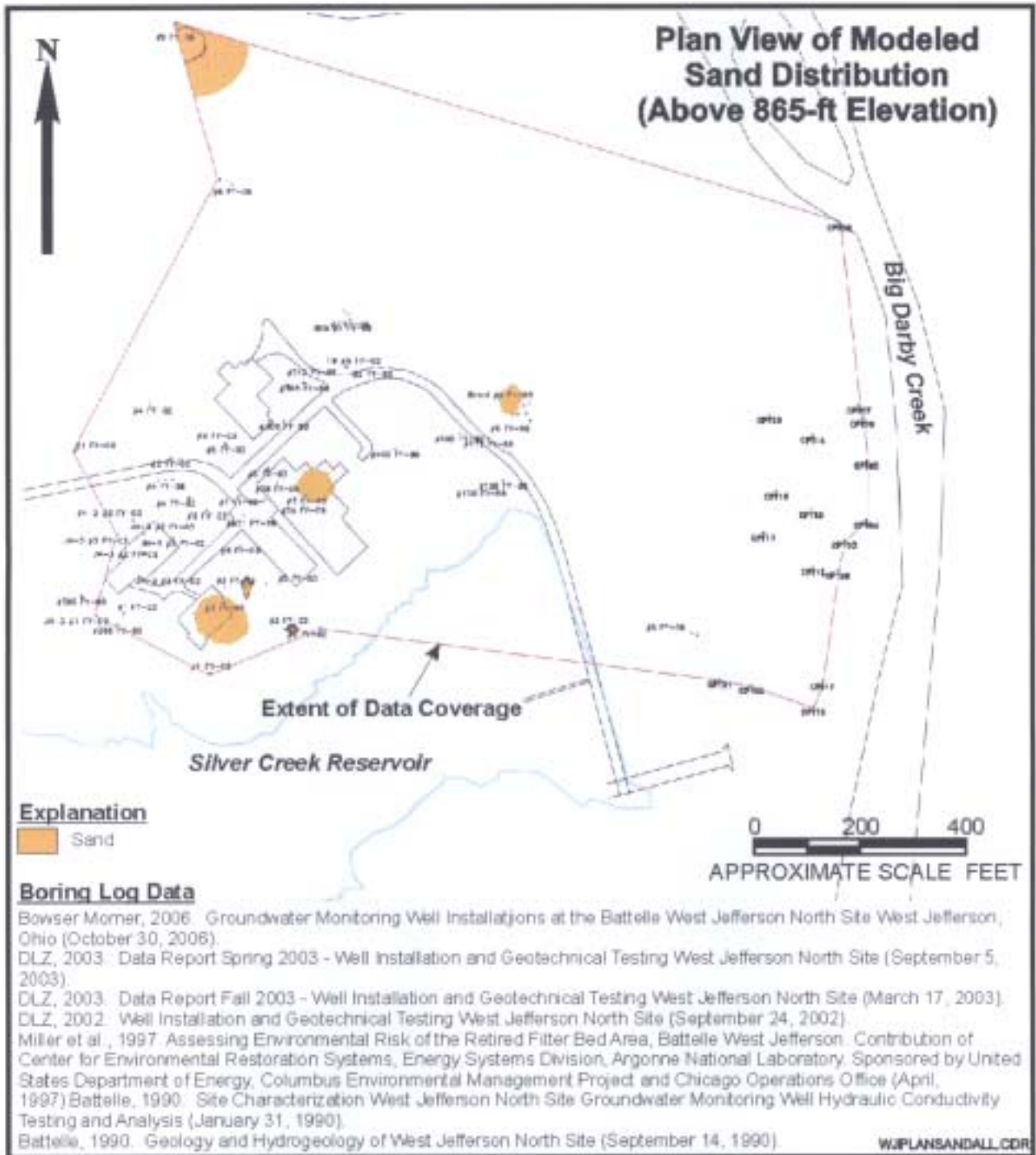


Fig 4a. Modeled Distribution of Sand/Gravel in Glacial Overburden Above 865-ft, amsl Based on Boring Log Data – Contouring Option 1

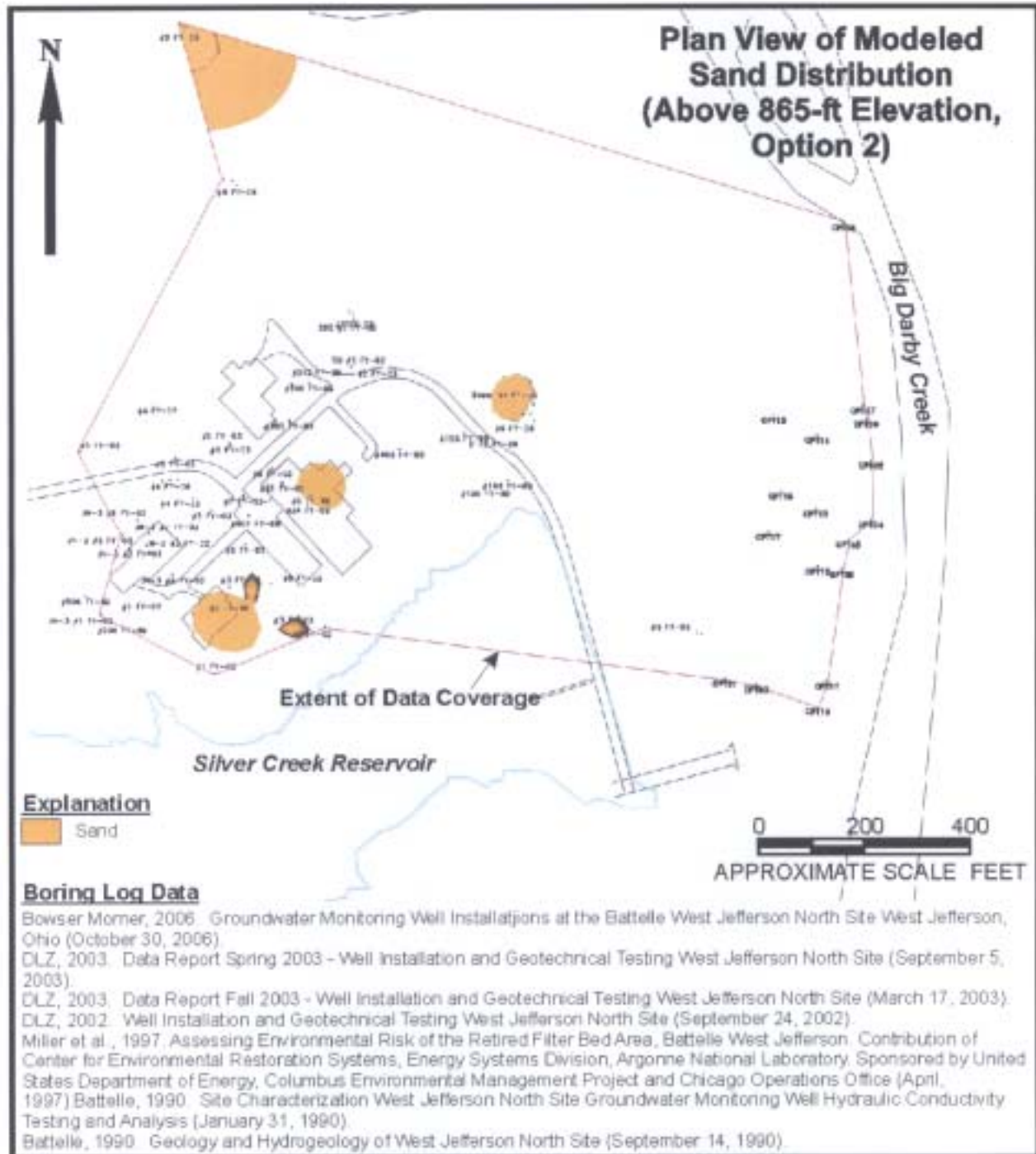


Fig 4b. Modeled Distribution of Sand/Gravel in Glacial Overburden Above 865-ft, amsl Based on Boring Log Data – Contouring Option 2

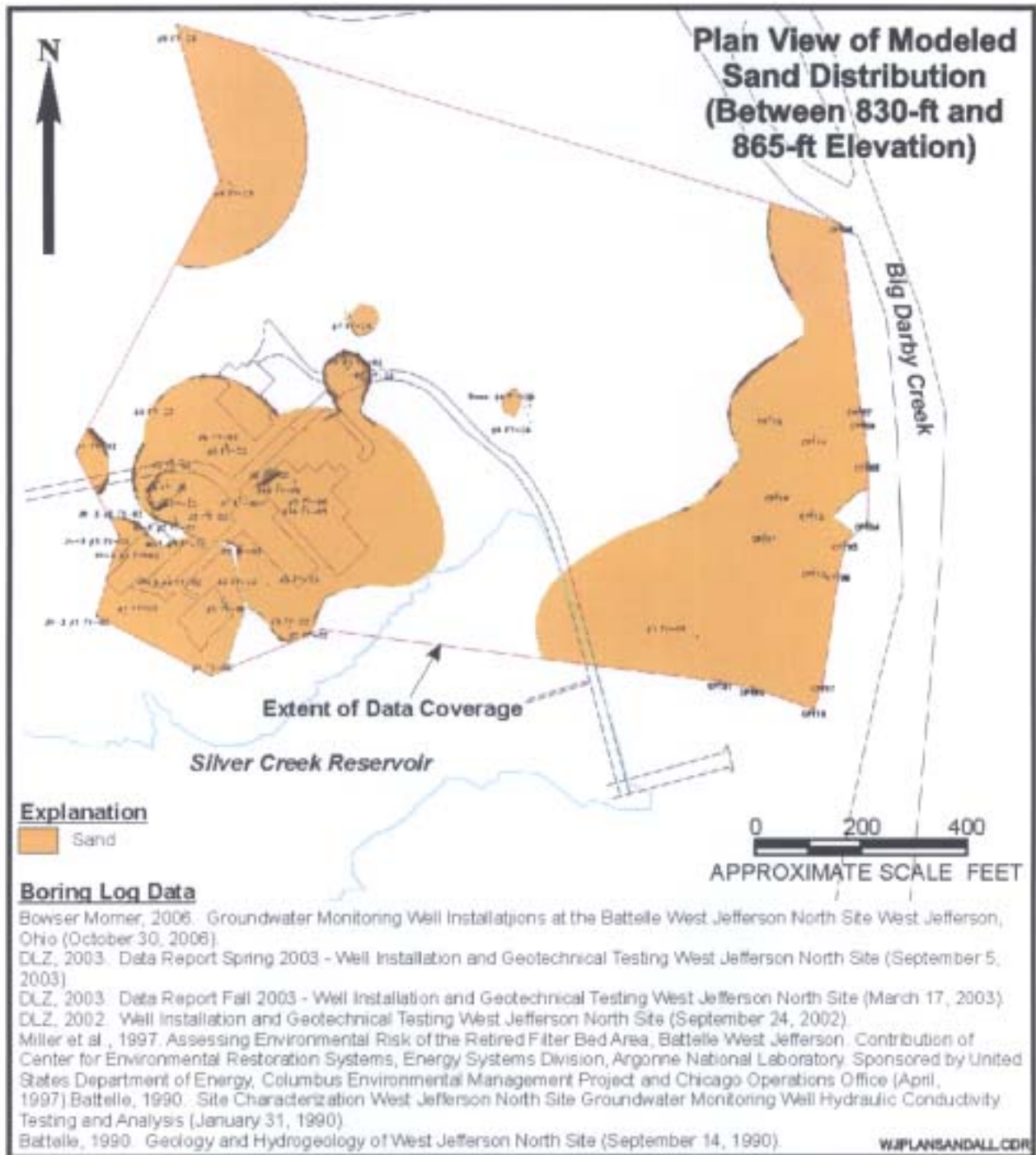


Fig 5a. Modeled Distribution of Sand/Gravel in Glacial Overburden Between 830 and 865-ft, amsl Based on Boring Log Data – Contouring Option 1

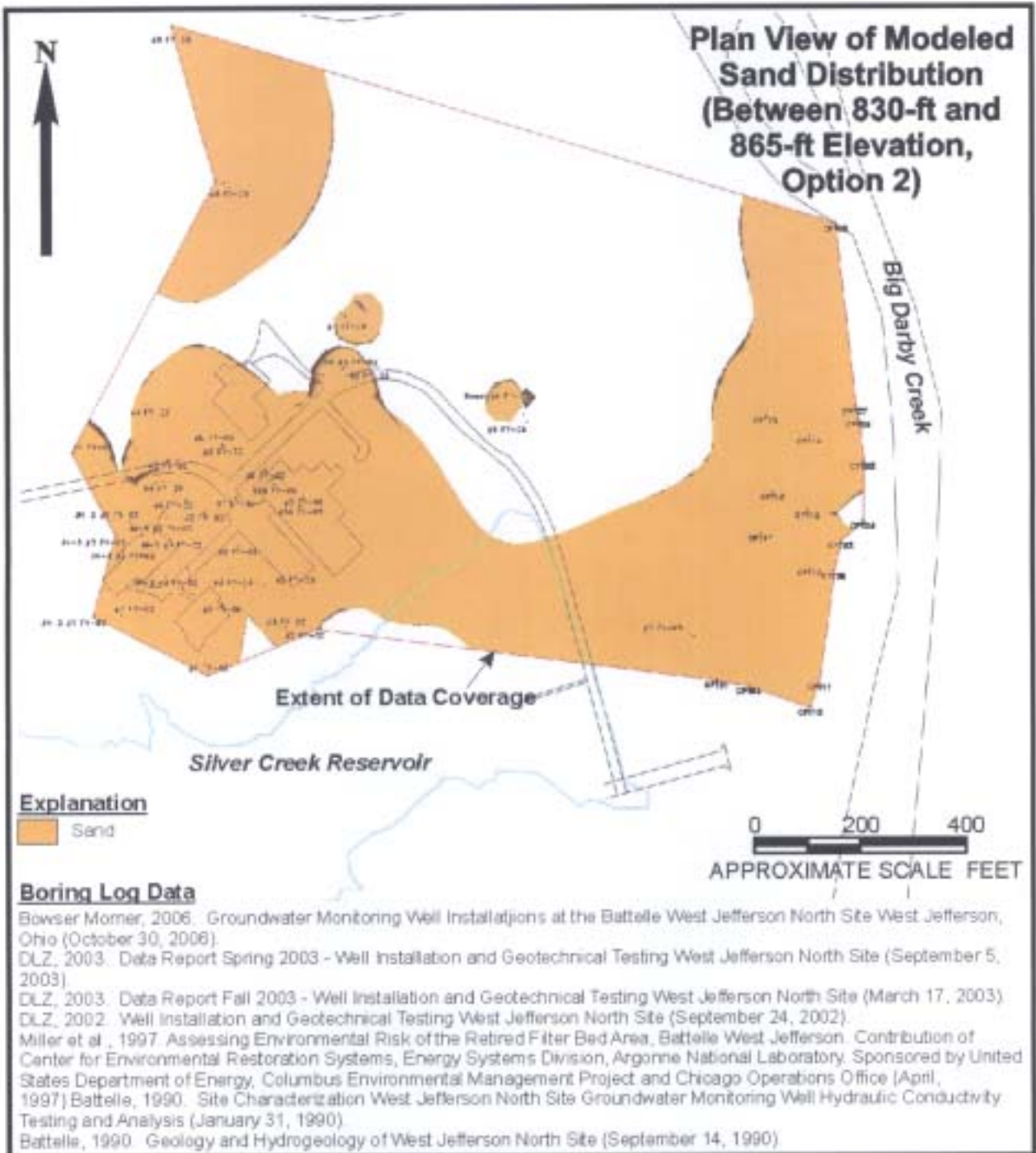


Fig 5b. Modeled Distribution of Sand/Gravel in Glacial Overburden Between 830 and 865-ft, amsl Based on Boring Log Data – Contouring Option 2

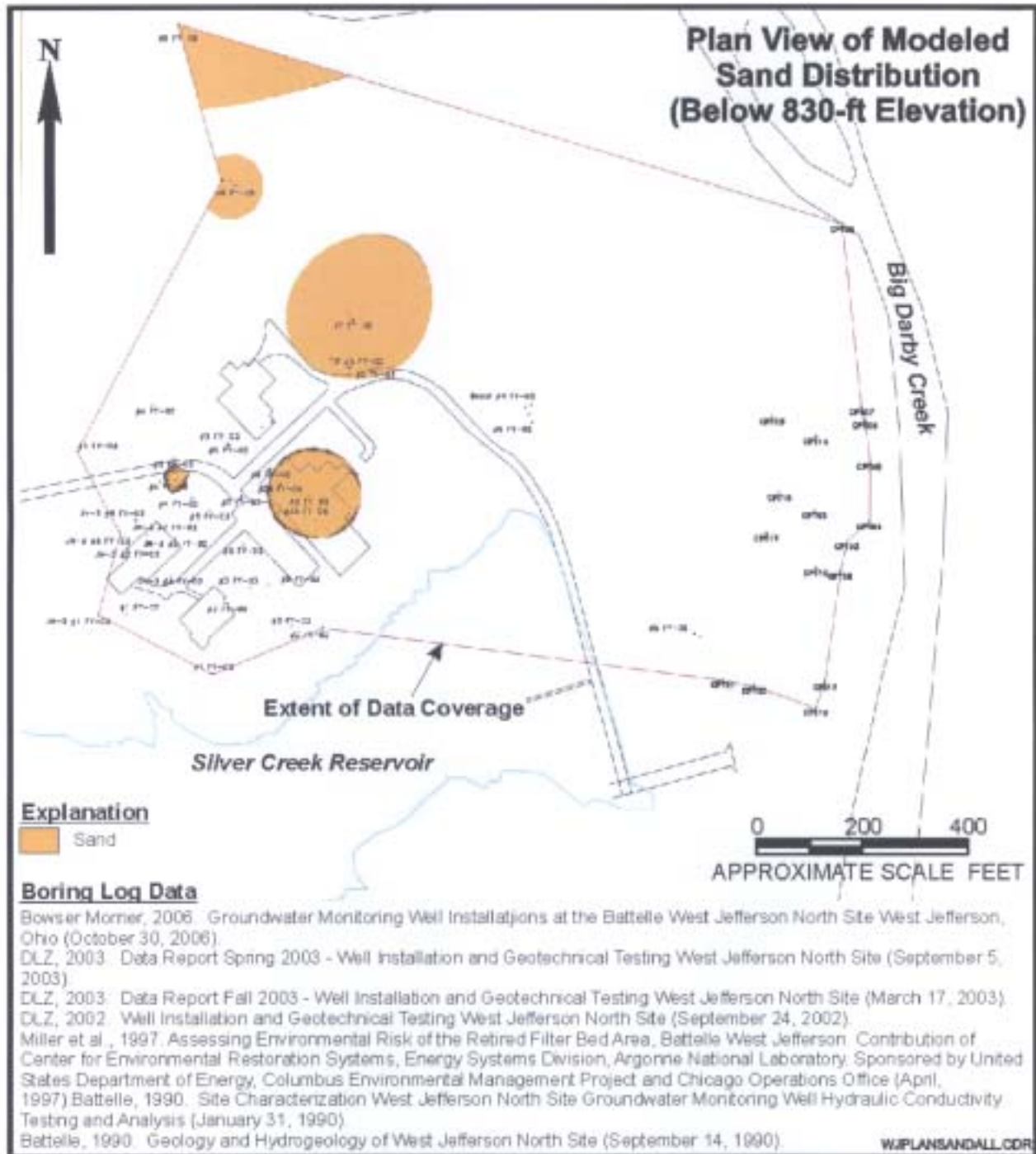


Fig 6a. Modeled Distribution of Sand/Gravel in Glacial Overburden Below 830 ft, amsl Based on Boring Log Data – Contouring Option 1

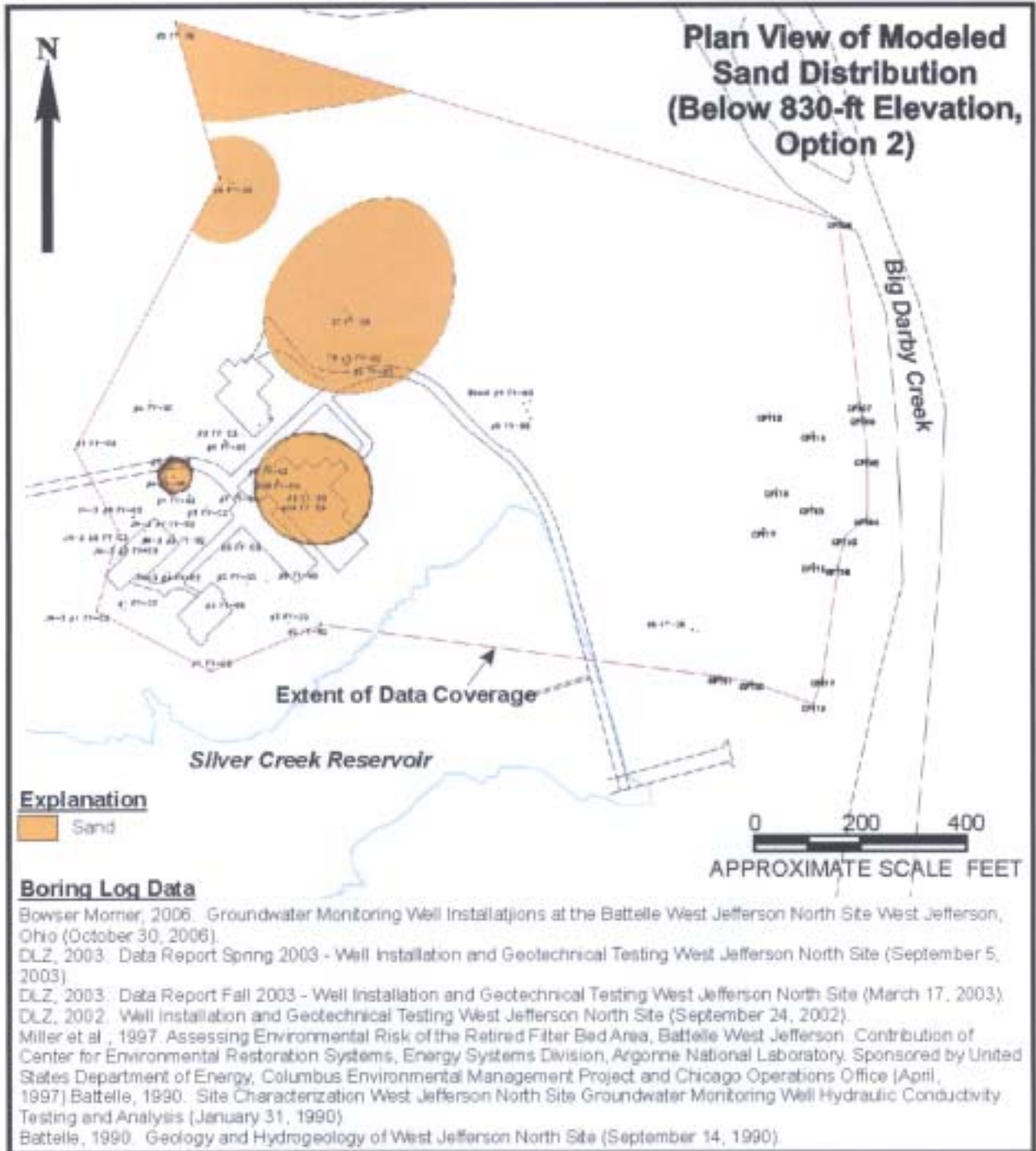


Fig 6b. Modeled Distribution of Sand/Gravel in Glacial Overburden Below 830 ft, amsl Based on Boring Log Data – Contouring Option 2

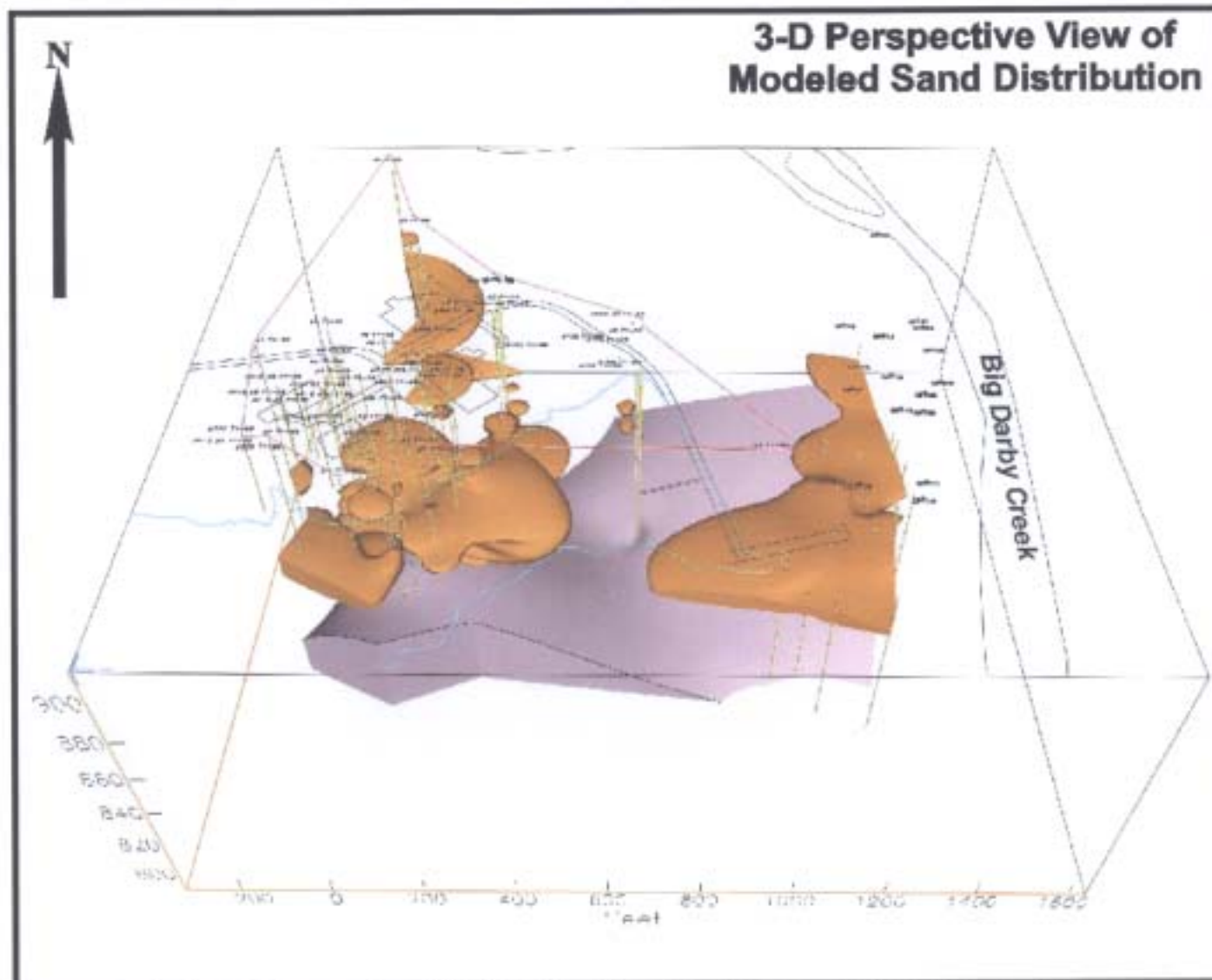


Fig 7a. 3D Perspective of Modeled Sand/Gravel Distribution in Glacial Overburden –
Contouring Option 1

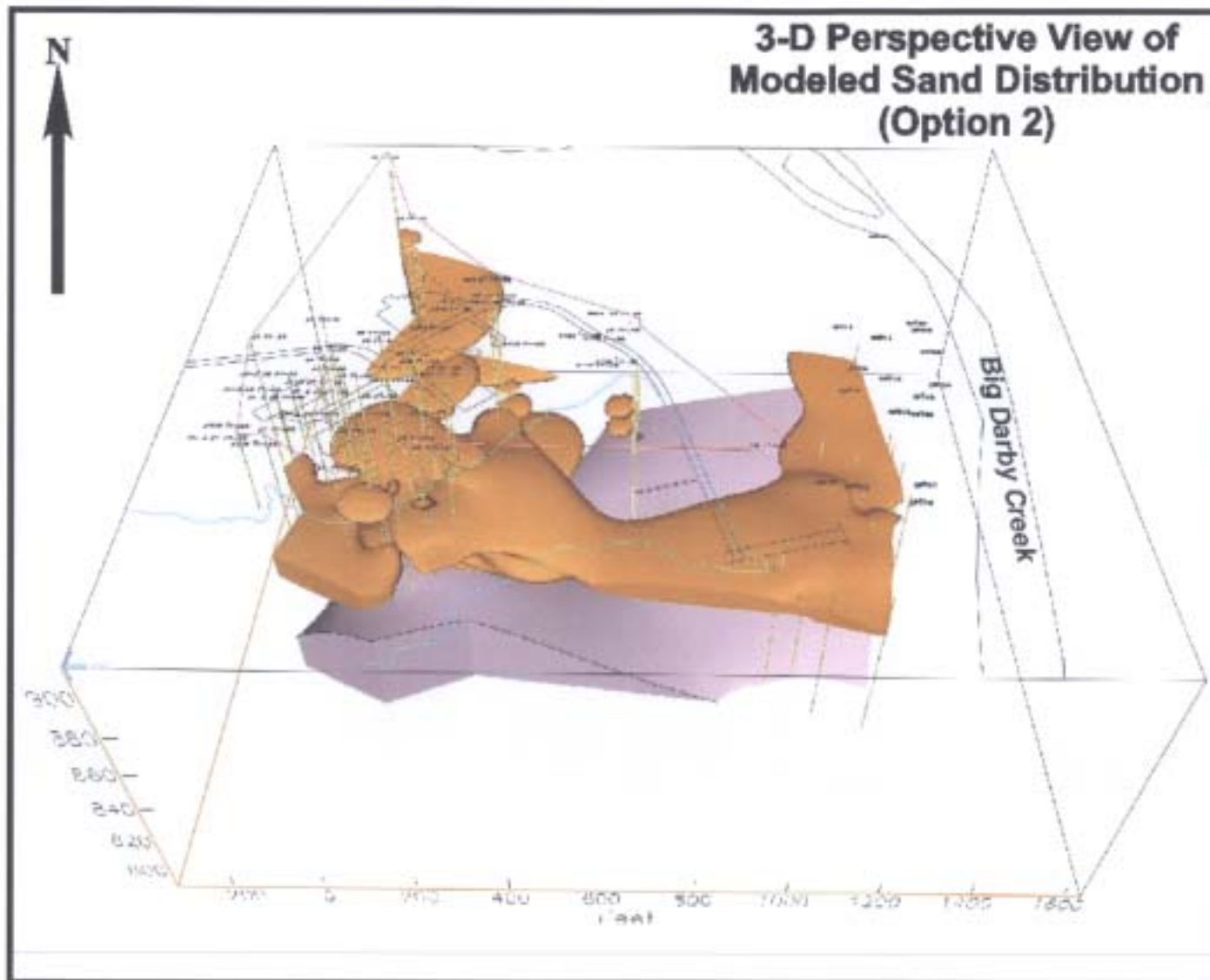


Fig 7b. 3D Perspective of Modeled Sand/Gravel Distribution in Glacial Overburden –
Contouring Option 2

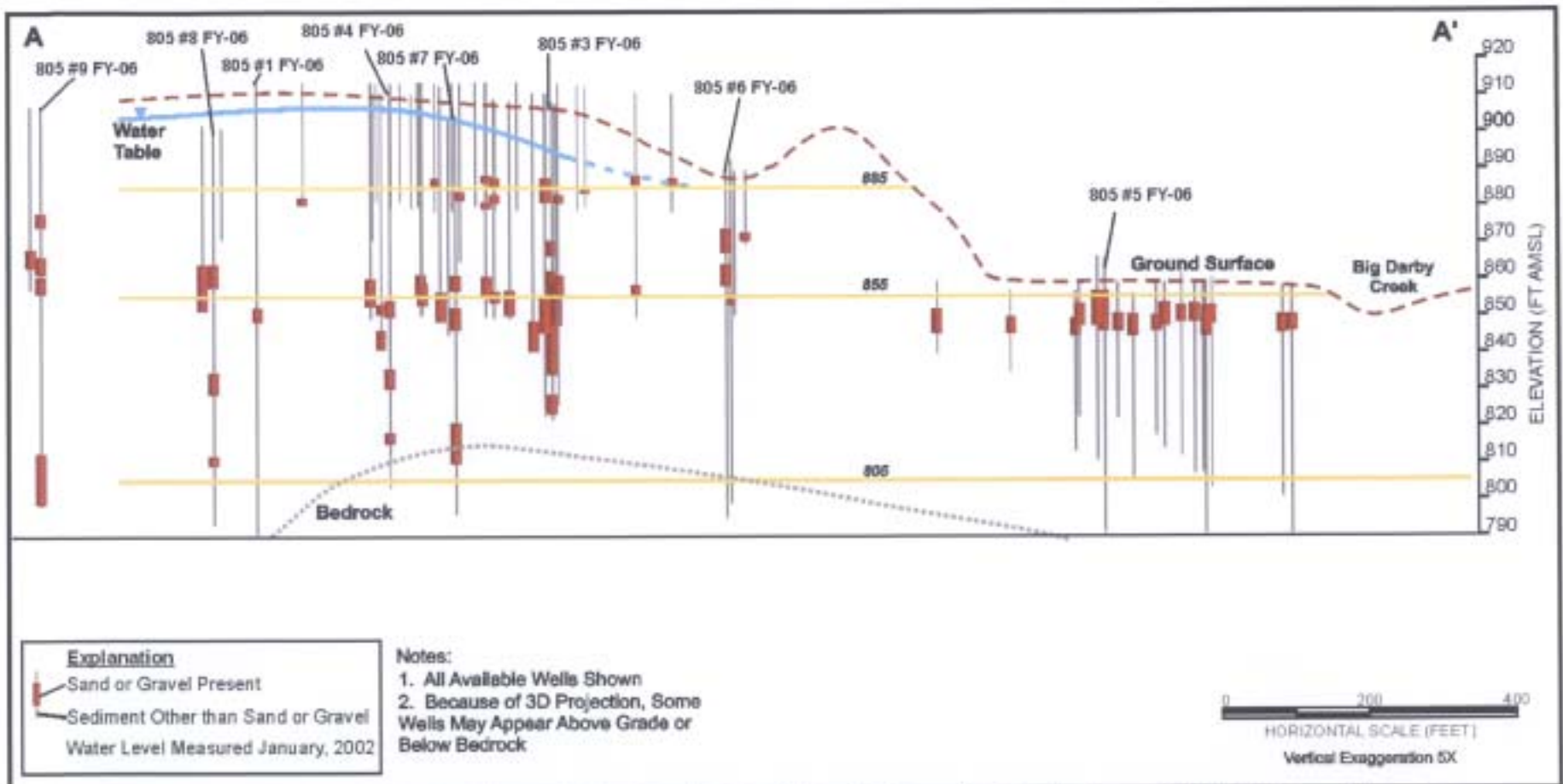


Fig 8. Composite Cross Section Through Site Showing Sand/Gravel Detected in Boring Logs (All Soil Borings Shown)

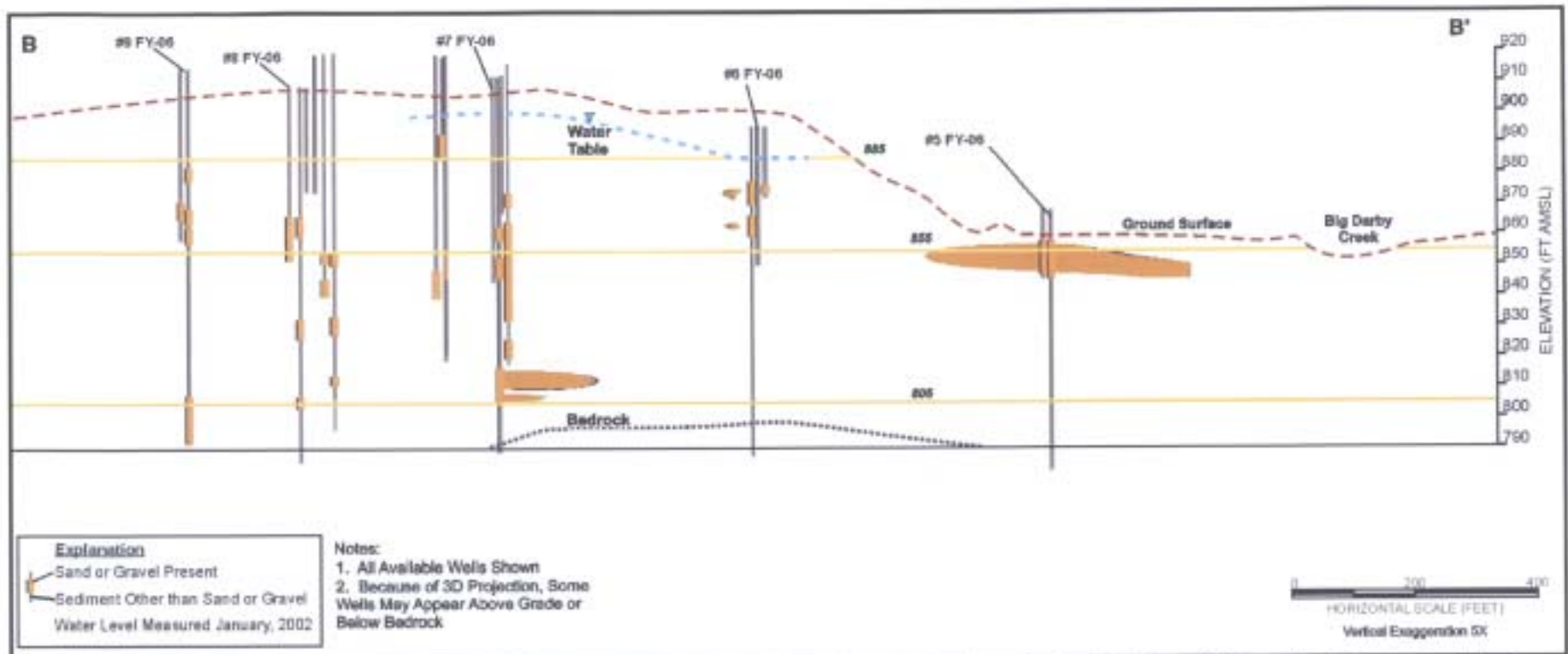


Fig 9a. Cross Section B-B' Showing Modeled Distribution of Sand/Gravel – Contouring Option 1 (Note: this Section Crosses the Site in the Same Location As OEPA Cross Section NW-SE)

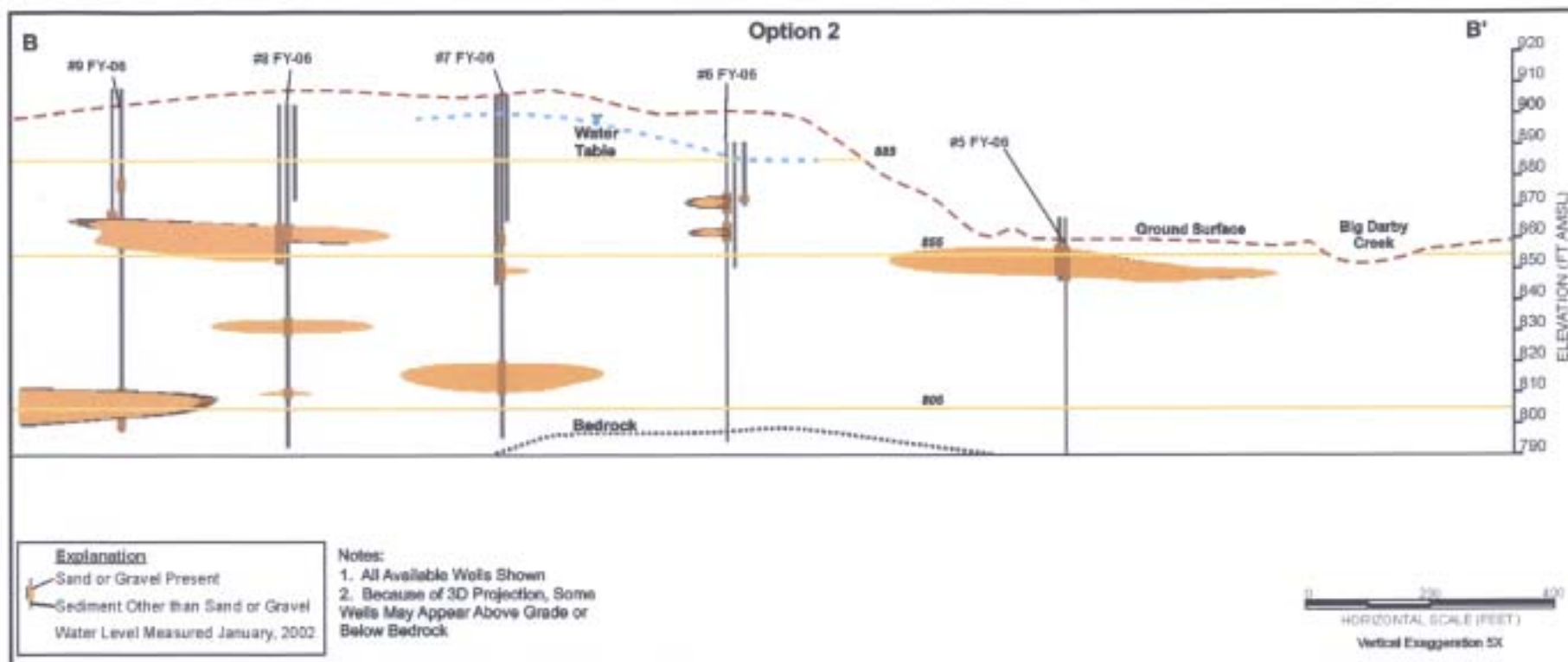


Fig 9b. Cross Section B-B' Showing Modeled Distribution of Sand/Gravel – Contouring Option 2 (Note: this Section Crosses the Site in the Same Location As OEPA Cross Section NW-SE)

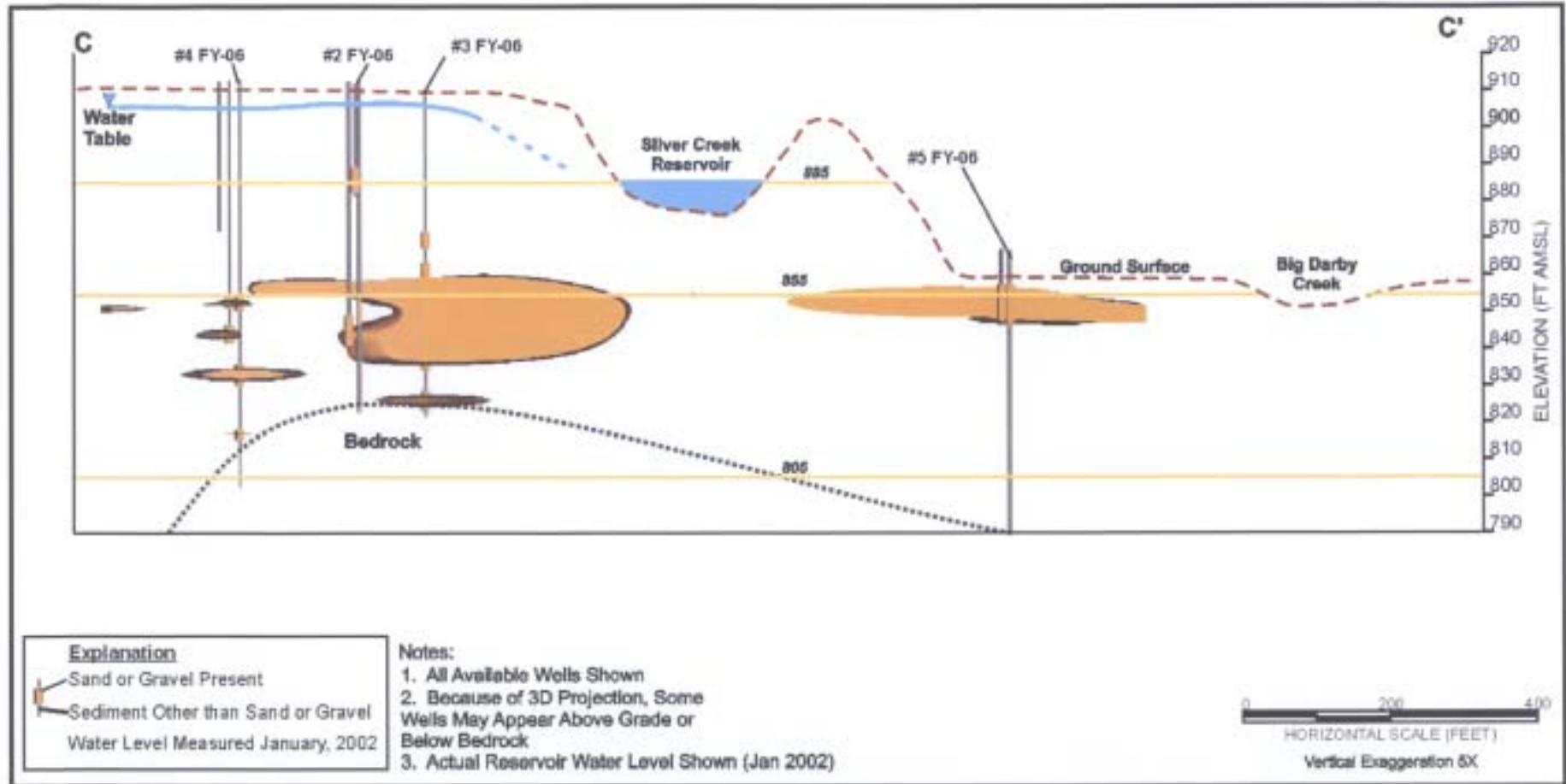


Fig 10a. Cross Section C-C' Showing Modeled Distribution of Sand/Gravel – Contouring Option 1 (Note: this Section Crosses the Site in the Same Location As OEPA Cross Section W-E)

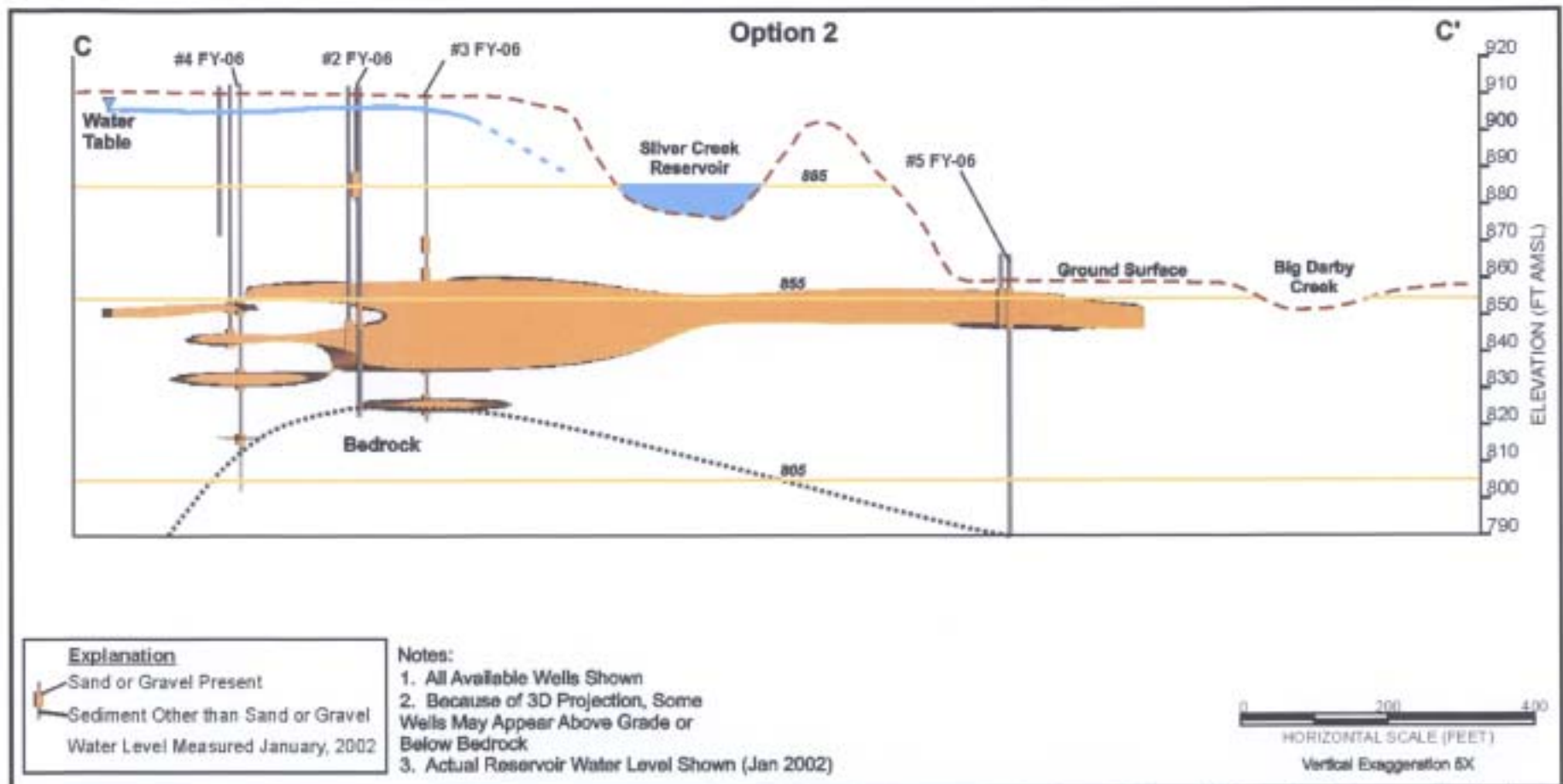


Fig 10b. Cross Section C-C' Showing Modeled Distribution of Sand/Gravel – Contouring Option 2 (Note: this Section Crosses the Site in the Same Location As OEPA Cross Section W-E)

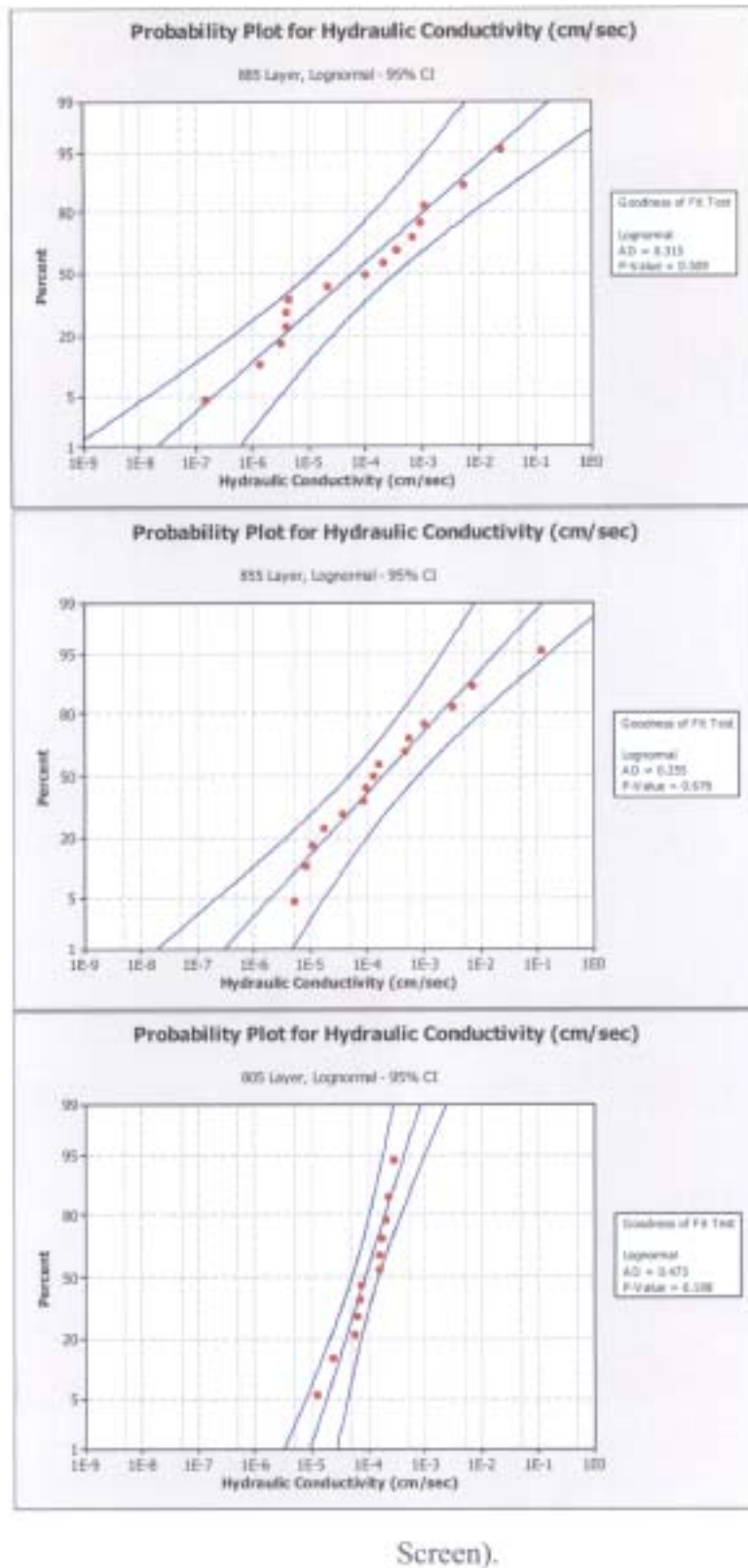


Fig 11.
Probab
ility Distribution
Plots of
Hydraulic
Conductivity
Data (Results
Segregated into
Three Groups
Based on
Elevation of
Monitoring Well
Screen).

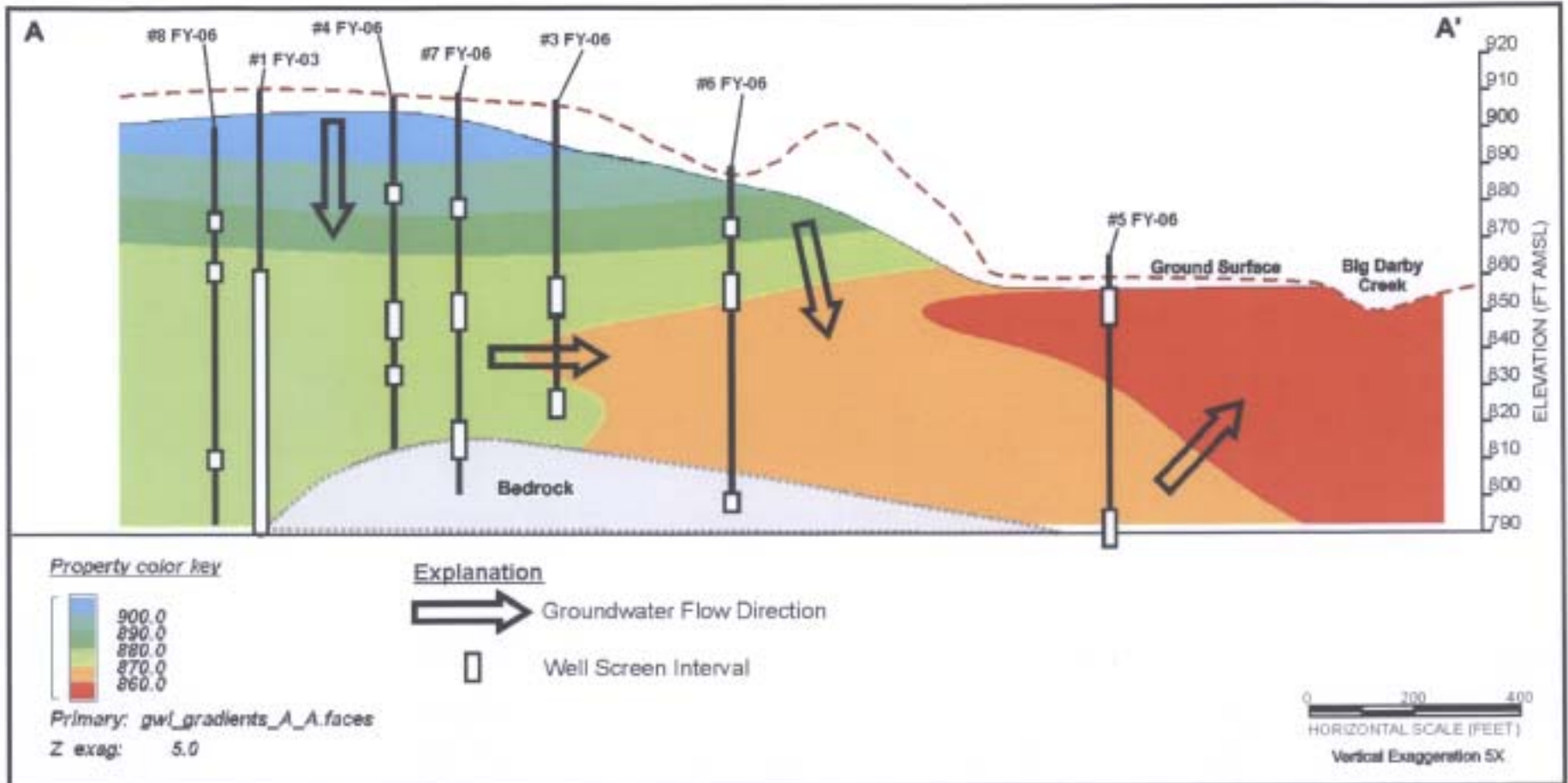


Fig 12. Cross Section Through Site Showing Direction of Groundwater Movement (Based on Water Level Measurements Collected October, 2007)